

# Free Radical Generation and Concentration in a Plasma Polymer: The Effect of Aromaticity

Sergey Ershov,<sup>†</sup> Farid Khelifa,<sup>‡</sup> Vincent Lemaur,<sup>§</sup> Jérôme Cornil,<sup>§</sup> Damien Cossement,<sup>||</sup> Youssef Habibi,<sup>‡,⊥</sup> Philippe Dubois,<sup>‡,||</sup> and Rony Snyders<sup>\*,†,||</sup>

<sup>†</sup>Chimie des Interactions Plasma Surfaces, Center of Innovation and Research in Materials and Polymers (CIRMAP), University of Mons (UMONS), Place du Parc 23, 7000 Mons, Belgium

<sup>‡</sup>Laboratory of Polymeric and Composite Materials, Center of Innovation and Research in Materials and Polymers (CIRMAP), University of Mons (UMONS), Place du Parc 23, 7000 Mons, Belgium

<sup>§</sup>Laboratory for Chemistry of Novel Materials, Center of Innovation and Research in Materials and Polymers (CIRMAP), University of Mons (UMONS), Place du Parc 23, 7000 Mons, Belgium

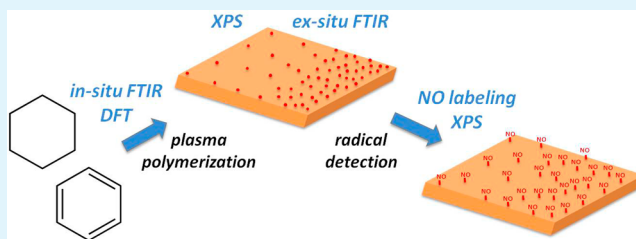
<sup>||</sup>Materia Nova Research Center, Parc Initialis, Avenue N. Copernic 1, 7000 Mons, Belgium

## Supporting Information

**ABSTRACT:** Plasma polymer films (PPF) have increasing applications in many fields due to the unique combination of properties of this class of materials. Among notable features arising from the specifics of plasma polymerization synthesis, a high surface reactivity can be advantageously used when exploited carefully. It is related to the presence of free radicals generated during the deposition process through manifold molecular bond scissions in the energetic plasma environment.

In ambient atmosphere, these radicals undergo autoxidation reactions resulting in undesired polymer aging. However, when the reactivity of surface radicals is preserved and they are put in direct contact with a chemical group of interest, a specific surface functionalization or grafting of polymeric chains can be achieved. Therefore, the control of the surface free radical density of a plasma polymer is crucially important for a successful grafting. The present investigation focuses on the influence of the hydrocarbon precursor type, aromatic vs aliphatic, on the generation and concentration of free radicals on the surface of the PPF. Benzene and cyclohexane were chosen as model precursors. First, in situ FTIR analysis of the plasma phase supplemented by density functional theory calculations allowed the main fragmentation routes of precursor molecules in the discharge to be identified as a function of energy input. Using nitric oxide (NO) chemical labeling in combination with X-ray photoelectron spectroscopy analysis, a quantitative evaluation of concentration of surface free radicals as a function of input power has been assessed for both precursors. Different evolutions of the surface free radical density for the benzene- and cyclohexane-based PPF, namely, a continuous increase versus stabilization to a plateau, are attributed to different plasma polymerization mechanisms and resulting structures as illustrated by PPF characterization findings. The control of surface free radical density can be achieved through the stabilization of radicals due to the proximity of incorporated aromatic rings. Aging tests highlighted the inevitable random oxidation of plasma polymers upon exposure to air and the necessity of free radical preservation for a controlled surface functionalization.

**KEYWORDS:** plasma polymerization, plasma phase FTIR, surface free radical density, chemical derivatization, plasma polymer aging



## INTRODUCTION

Plasma-based approaches for the synthesis of polymer-like thin films continue to attract considerable attention in fields such as microelectronics, optics, food packaging, and, particularly, in biomedicine.<sup>1–6</sup> The synthesis technique, i.e., plasma-enhanced chemical vapor deposition (PECVD), relies on the principles of competitive ablation polymerization (CAP), initially developed by Yasuda<sup>7,8</sup> and subjected recently to a number of excellent reviews.<sup>9,10</sup> The mechanism of plasma polymer growth is responsible for the unique properties of this class of materials. Plasma polymer films (PPF) can be deposited in a range of thicknesses from nano- to micrometer scale; they exhibit good adhesion to various substrates, including ceramics and metals;

the pinhole free, profoundly branched and cross-linked structure (howbeit tunable depending on deposition conditions so that it may, to a certain degree, retain the original precursor units<sup>11,12</sup>) provides a remarkable thermal and chemical stability for an organic-like material. The feature of interest in the current work, a highly reactive PPF surface rich in free radicals, is a direct consequence of the plasma polymerization mechanism that is extremely different from classical polymerization methods. It entails manifold composite physicochemical

Received: April 14, 2014

Accepted: June 30, 2014

Published: June 30, 2014

reactions and is, very briefly speaking, based on the fragmentation of an organic precursor by means of a plasma with an average electron energy of 2–5 eV and on the polyrecombination of thereby generated reactive species into a growing film on the substrate. Upon condensation on the substrate, a major part of radicals randomly recombines to form a hyper-branched and cross-linked three-dimensional network while the other part gets trapped in it, and thus survives in the bulk and on the surface of the plasma polymer. When removed out of the vacuum chamber into the ambient, plasma polymers encounter the widely reported aging problem.<sup>13,14</sup> Omnipresent oxygen molecules react with surface free radicals and form initially well-defined chemical functionalities, which on a longer time-scale of oxidation, also referred to as autoxidation,<sup>15</sup> randomly convert to a large variety of oxygen-containing groups. They dominate over the PPF surface, causing its uncontrollable functionalization and thus complicating the efficiency and selectivity of the originally intended functionalization.

However, once the plasma polymer synthesis or plasma-treatment process is completed, the surface free radicals can survive rather long in anaerobic conditions while retaining a highly reactive surface.<sup>16</sup> This reactivity may be advantageously exploited for a controlled grafting of a specific chemical group or molecule (plasma-induced grafting). Thus, in order to preserve as much as possible radicals from postoxidation, the functionalization step should take place under vacuum without air exposure. Although numerous reports of grafting on plasma-treated polymer surfaces can be found, e.g., acrylic acid or acrylamide groups incorporated on Ar-treated poly(ether sulfone) membranes,<sup>17,18</sup> such reports are rather scarce in the case of plasma-synthesized polymers. For instance, the grafting and polymerization of styrene on maleic anhydride-based plasma polymer<sup>19</sup> and of 2-ethylhexyl acrylate on isopropyl alcohol-based plasma polymer<sup>20</sup> are among the very few examples that have been reported.

In the context of a plasma-induced grafting procedure, it is evident that the surface free radical density is an important parameter because, e.g., too few radicals might lead to an incomplete coverage of the PPF with desired functional groups. There are several well-established chemical and physical methods of surface radical identification and quantification, such as electron spin resonance (ESR) or chemical derivatization with 2,2-diphenyl-1-picrylhydrazyl (DPPH), each with its own pros and cons.<sup>15,21,22</sup> The method of radical labeling with nitric oxide (NO) and subsequent nitrogen detection by an X-ray photoelectron analysis (XPS) has proven to be a very efficient technique for radical detection due to a prompt recombination of NO molecules with even weakly reactive radicals on the PPF surface and due to the easiness of gaseous chemical agent introduction into the vacuum chamber. This method was extensively employed by Wilken and co-workers in order to study the reactive surface of plasma treated polyethylene (PP)/polypropylene (PE)<sup>23,24</sup> and was recently adapted for the current work.<sup>25</sup>

The versatility of plasma polymerization stems from the possibility to employ almost any organic precursor (given that it can be easily introduced as vapor into the vacuum chamber) for the synthesis of a polymer-like material. However, the precursor type might affect fragmentation patterns in plasma and, hence, the radical generation and concentration closely related with the grafting potential. Although there are numerous studies on the effect of precursor saturation on

generation, concentration and stability of surface free radicals,<sup>15,16,23,26</sup> only a few works deal with free radical detection and their role in the plasma polymer formation from aromatic precursors or in plasma-treated aromatic polymers. For instance, Kuzuya et al.<sup>27</sup> studied free radicals in powdered Ar-irradiated polystyrene with the help of ESR. Different types of resonance-stabilized radicals were identified and their recombination routes, resulting in increased cross-linking, were proposed. Kosobrodova et al.<sup>28</sup> has investigated N<sub>2</sub>-plasma treated polystyrene by ESR, identified different types of C-centered free radicals and proposed a model of structure transformations based on free radical decay kinetics. Concerning plasma polymers, Meyer-Plath, in a review on free radical detection techniques,<sup>15</sup> has made a brief reference to the results of their group concerning plasma polymers synthesized from aromatic precursors, styrene, and toluene. The surface free radical density, evaluated by NO derivatization, served solely as an example to demonstrate the effect of precursor unsaturation on the free radical concentration without a detailed PPF characterization. Yamauchi et al.<sup>16</sup> compared ESR intensities for plasma polymers deposited from several simple precursors, including benzene, both in anaerobic and aerobic conditions. The authors conclude that the precursor unsaturation can strongly influence the amount of free radicals and their stability toward quenching with oxygen. However, in the covered power range, only one type of free radical was detected and potential resonance-stabilized free radicals arising from benzene were not observed.

A profound understanding of the correlation between the aromatic nature of the precursor and the free radical generation mechanism in plasma (including the generation of resonance-stabilized free radicals) and their concentration in the plasma polymer is yet to be achieved. On the basis of these considerations, the aim of our work is to contribute toward this understanding through a thorough free radical investigation of PPF synthesized from two simple organic molecules, benzene, and cyclohexane, presenting aromatic and aliphatic C–C bonding, respectively. A complete study of free radical generation and their surface concentration in dependence on the hydrocarbon precursor type is proposed. Insights into the plasma polymer formation mechanisms for the two precursors in combination with the quantitative evaluation of the surface free radical density provided essential information for a successful future functionalization of the PPF. Fragmentation patterns of original precursor molecules in the discharge were addressed by in situ Fourier transform infrared spectroscopy (FTIR) and supported further by density functional theory (DFT) calculations. The comparison of plasma phase FTIR spectra with those of the deposited films linked the discharge and the synthesized material characterization and gave a valuable insight into the mechanisms of polymer generation. The PPF structure was additionally studied by XPS analysis. The density of surface free radicals was quantitatively evaluated by NO chemical derivatization in combination with XPS analysis and interpreted considering the entire set of characterization findings. Aging tests, represented as the oxygen uptake and the free radical decay upon air exposure, allowed to investigate the surface reactivity of the PPF and its potential for further functionalization once removed from the vacuum chamber into the ambient.

## EXPERIMENTAL SECTION

PPF were synthesized by PECVD on p-type (B-doped) Si substrates (acetone/methanol precleaned) with benzene (analytical purity, UCB) and cyclohexane (analytical purity, Acros Organics) gas in a lab-scale deposition chamber. The distance between the inductive coil, powered by a CESAR 1310 generator from Advanced Energy, and the substrate was fixed at 5.5 cm. Evacuating the chamber by a combination of scroll and turbomolecular pumps allowed a base pressure on the order of  $10^{-4}$  Pa to be obtained. The working pressure of 6.67 Pa was kept constant by a throttle valve while the amount of precursor gas was controlled by a mass flow controller. PPF depositions with 15 sccm of precursor gas were carried out in the range of input powers 75–400 W giving rise to varying thicknesses measured by a mechanical profilometer Dektak 150 from Veeco.

Immediately after the synthesis PPF, samples were transferred into a separate vacuum chamber (base pressure  $<10^{-3}$  Pa) for derivatization tests without exposure to the ambient atmosphere (see Figure 1 for

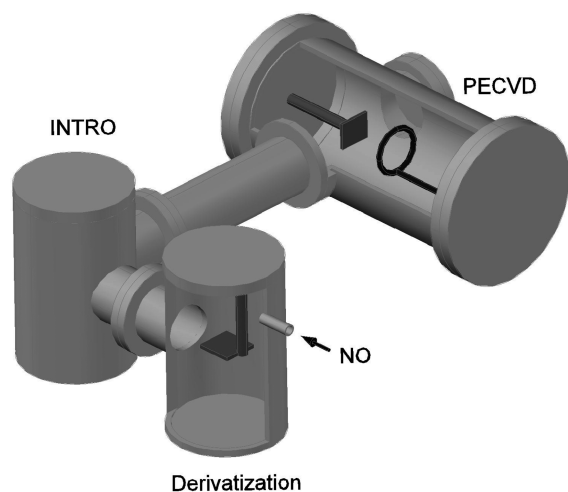


**Figure 1.** Schematic drawing of PECVD and derivatization chambers.

the set of PECVD and derivatization chambers). The transfer under vacuum (pressure around  $10^{-4}$  Pa) took  $\sim 2$  min. The labeling agent, nitric oxide NO (Air Liquide, 99.9%), was introduced into the chamber until the desired pressure (Pirani gauge controlled) was attained under static conditions (turbo pump blocked using a gate

valve). The derivatization pressure of  $10^4$  Pa and time of 15 min have been optimized in a previous work.<sup>25</sup>

Plasma diagnostic of the benzene/cyclohexane discharge by an in situ FTIR spectroscopy was performed with an Agilent 670 FTIR spectrometer aligned with a multireflection mirror system and mounted directly to the deposition chamber. Thirteen mirrors, resulting in an optical path length of 26 m, allow for a sufficient signal-to-noise ratio to be accumulated due to the multiple passes of the beam through the plasma. Spectra from 600 to  $4000\text{ cm}^{-1}$  were recorded with a resolution of  $4\text{ cm}^{-1}$  and averaged over 64 scans. For data treatment, the Blackman Harris 4 Term apodization function was applied.

The ground-state geometry of the molecules has been optimized at the density functional theory (DFT) level using the B3LYP functional and the 6-311++G(3df,3pd) basis set. Energy minima have been systematically confirmed through a vibrational frequency analysis. For reactions involving biradicals, both singlet and triplet states were optimized and only the most stable structure was considered for calculating the Gibbs free energies of the reaction. The later were obtained by subtracting the free energy of the reactants to the energy of the products. Our study thus only focuses on thermodynamic aspects because the activation energies are not estimated. Indeed, single bond cleavages are known to be barrierless processes whereas activation energies associated with rearrangement reactions of small molecules are smaller than bond cleavages energies so that rearrangement reactions will occur if single bond cleavages do.<sup>29,30</sup> All the calculations have been performed within the Gaussian09 package.<sup>31</sup>

Synthesized PPF samples were investigated by ex situ FTIR spectroscopy using an Excalibur FTS 3000 FTIR spectrometer from Bio-RAD in attenuated total reflection (ATR) mode. Spectra from 600 to  $4000\text{ cm}^{-1}$  were recorded with a resolution of  $4\text{ cm}^{-1}$  and averaged over 32 scans. Notably thick films ( $3\text{ }\mu\text{m}$ ) were produced in order to accumulate a good signal-to-noise ratio.

The chemical composition of the PPF was evaluated by XPS on a VERSAPROBE PHI 5000 hemispherical analyzer from Physical Electronics with a base pressure of  $<3 \times 10^{-7}$  Pa. The X-ray photoelectron spectra were collected at a takeoff angle of  $45^\circ$  with respect to the electron energy analyzer, operating in constant analyzer energy (CAE) mode (11.75 eV). The spectra were recorded with monochromatic Al  $K\alpha$  radiation (15 kV, 25 W) with a highly focused beam size of  $100\text{ }\mu\text{m}$ . The energy resolution was 0.7 eV. The binding energy scale of the spectra was calibrated with respect to the aliphatic component of the C 1s peak at 285 eV.<sup>32</sup> Possible surface charging was compensated by a built-in electron gun and an argon ion neutralizer. N

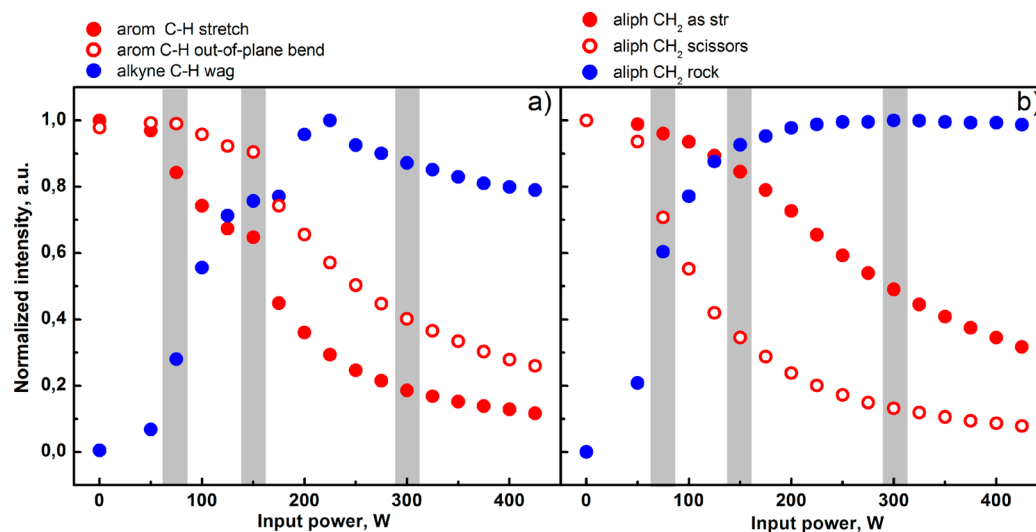


**Figure 2.** Normalized intensities of selected IR bands for the benzene (a) and cyclohexane (b) plasma as a function of input power with highlighted power values for PPF characterization.

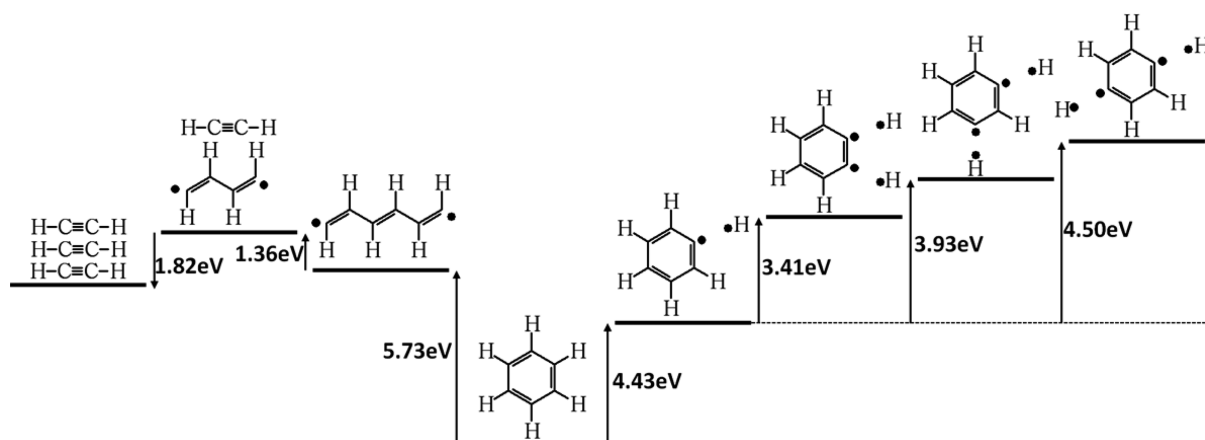


**Figure 3.** DFT-calculated (B3LYP/6-311++G(3df,3pd) Gibbs free energies (in eV) of different homolytic C–H and C–C bond breakings.

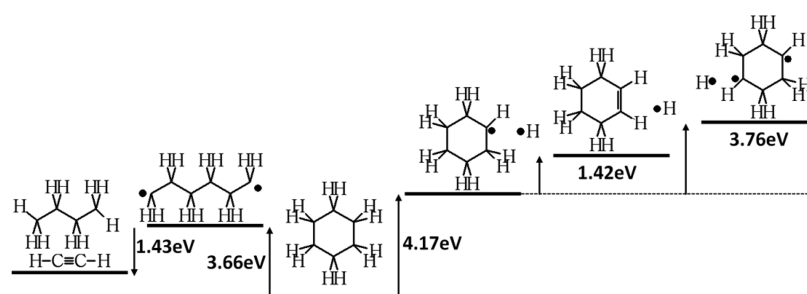


**Figure 4.** DFT-calculated (B3LYP/6-311++G(3df,3pd) Gibbs free energies (in eV) of different homolytic C–H and C–C bond breakings.

Its spectra were recorded with a high pass energy (58.7 eV) in order to reduce the acquisition time and to avoid degradation of some  $\text{NO}_x$  compounds and at the same time to obtain a good signal-to-noise ratio essential for the data analysis of very small amounts of nitrogen.

## RESULTS AND DISCUSSION

**Comparison of Plasma Polymerization of Benzene and Cyclohexane.** To study the generation of surface free radicals in the PPF, the strategy of selecting conditions corresponding to distinctive degrees of the precursor fragmentation in plasma, followed by the detailed characterization of the respective films has been adopted. With the help of in situ FTIR spectroscopy of the plasma phase, fragmentation patterns for the benzene and cyclohexane precursors were explored through tracing the IR band intensities of the original molecules and fragmentation products as a function of input power in the range 50–300 W. The procedure of in situ FTIR measurements for benzene and cyclohexane discharges as well as a table listing FTIR group wavenumbers (literature<sup>33–35</sup>) and absorbance-peak centers (experimental) of the most intense vibrational bands observed in plasma and in solid PPF samples are presented in the Supporting Information.

After the recording of spectra from the benzene and cyclohexane discharges and IR peak attribution,<sup>33–35</sup> the normalized intensities of three bands, corresponding to two characteristic bands of the precursor and to one new band observed in plasma, have been plotted for each precursor as a function of power (Figure 2).

For the benzene precursor, both high intensity IR bands characteristic of the unfragmented molecule, namely, aromatic C–H stretch (peak at  $\sim 3047\text{ cm}^{-1}$ ) and out-of-plane C–H bend (peak at  $\sim 672\text{ cm}^{-1}$ ), decrease with power. A

discontinuity observed around 175 W may be attributed to the transition between capacitive and inductive modes of plasma generation in an inductively coupled discharge, as investigated in detail in a plasma polymerization study of propanethiol.<sup>36</sup> Along with the decrease of original band intensities, a new band, attributed to alkyne C–H wag (peak at  $\sim 729\text{ cm}^{-1}$ ), appears and grows in the course of fragmentation, reaching its maximum at around 225 W. For a better interpretation of the in situ FTIR patterns, the Gibbs free energies corresponding to different possible bond breakings in a benzene molecule have been estimated at the DFT level and are presented in Figure 3.

Considering the average electron energy of 2–5 eV for a typical plasma polymerization process<sup>8,37</sup> and combining the observed IR band interdependent changes with DFT calculations, it appears that the first energetically accessible fragmentation pathway is the homolytic C–H bond breaking from the original benzene molecule ( $\sim 4.4\text{ eV}$ ) producing activated aromatic free radicals. Increased energy input causes stronger fragmentation of the monomer, resulting in the opening of the benzene ring ( $\sim 5.7\text{ eV}$ ), which leads to further fragmentations into small-molecular fragments with predominating acetylenic species characterized at the IR level (Figure 2). Notable  $\text{C}_2\text{H}_2$  generation has already been reported for RF discharges of benzene.<sup>38,39</sup> Nevertheless, the aromatic free radical formation is favored over acetylene production at lower energies.

For the cyclohexane precursor, two original IR bands, namely, alkane asymmetric  $\text{CH}_2$  stretch (peak at  $\sim 2933\text{ cm}^{-1}$ ) and  $\text{CH}_2$  scissors (peak at  $\sim 1456\text{ cm}^{-1}$ ), exhibit an intensity reduction accompanied by the alkane  $\text{CH}_2$  rock band (peak at  $\sim 730\text{ cm}^{-1}$ ) growth. This band, absent in the original cyclohexane molecule, represents the  $\text{CH}_2$  rocking vibration



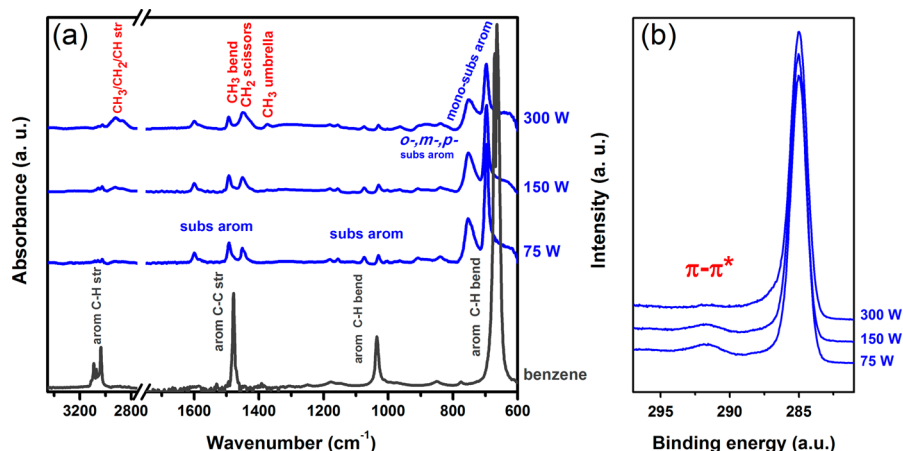


**Figure 5.** Ex situ FTIR (a) and C 1s XPS (b) spectra for the benzene-based PPF synthesized at different deposition powers.

of alkanes and occurs only for structures with four or more  $\text{CH}_2$  groups in a row.<sup>33</sup> Its observation for the lowest deposition power implies that, starting from 75 W, the provided energy is sufficient enough to break up a considerable amount of saturated rings into relatively long hydrocarbon fragments. This observation is also supported by the DFT estimation of Gibbs free energies corresponding to different possible bond breakings of a cyclohexane molecule, as presented in Figure 4.

The most energetically accessible fragmentation pathway is the opening of the aliphatic cycle ( $\sim 3.7$  eV) followed by its reorganization into more stable components, a long (four carbon atoms) hydrocarbon fragment and an acetylenic intermediate. The homolytic C–H bond breaking of the cyclohexane molecule is energetically more expensive ( $\sim 4.2$  eV) and, upon further H detachments, can produce a number of activated cyclohexane free radicals that eventually lose their identity in the condensed PPF due to multiple substitutions. The lower energy cost to open the cyclohexane ring ( $\sim 3.7$  eV) as compared to the alkyne formation for benzene ( $\sim 5.7$  eV) is confirmed by the relative intensities of the new IR bands observed for the power of 75 W (Figure 2), for benzene, the alkyne C–H wag exhibits only 30% of the max intensity whereas for the cyclohexane, the aliphatic  $\text{CH}_2$  rock already demonstrates 60% of the max intensity. Those less abundant ring openings for benzene in plasma result from the loss of electron delocalization that is energetically unfavorable.

The IR band–power dependencies, shown in Figure 2, were used as an initial guide in choosing conditions corresponding to minor, medium, and strong fragmentation of precursor molecules in plasma. When considering cyclohexane and benzene precursors, the input powers of 75, 150, and 300 W resulted in the approximately desired degrees of fragmentation as indicated by the respective IR band intensity changes of original bands and reaction products. Hence, the PPF deposited at these powers were studied thoroughly by ex situ FTIR and XPS in order to correlate the PPF structure with the free radical generation.

First, the structure of plasma polymers, synthesized at selected powers, was addressed by an ex situ solid phase FTIR analysis. Figure 5 shows FTIR and XPS spectra of the benzene-based PPF deposited with the input powers of 75, 150, and 300 W. The spectrum of liquid benzene is presented for comparative purposes.

The ex situ FTIR spectrum of the benzene-based PPF deposited at 75 W exhibits changes as compared to the pure

liquid benzene spectrum. Distinct bands attributed to intact rings in the original precursor molecule (ring modes, in-plane and out-of-plane C–H bends) transform in the PPF into multiple peaks associated with the mono-substitution of one hydrogen atom on the ring. For the lowest deposition power, as suggested by the DFT-calculated fragmentation scheme, the PPF structure presumably consists of phenyl rings joined randomly by short alkyl chains. Activated aromatic free radicals, produced through H abstraction, upon their condensation into the PPF, generate a free radical center from which a branch can grow. The higher energy input leads to the intensity reduction of aromatic bands accompanied by the appearance and growth of peaks in the group wavenumbers of saturated aliphatic hydrocarbons, namely, sym/assym C–H stretches ( $2820\text{--}2990$   $\text{cm}^{-1}$ ) and corresponding bends ( $1360\text{--}1470$   $\text{cm}^{-1}$ ). Additionally, small bands emerging in the region around  $700\text{--}900$   $\text{cm}^{-1}$  are associated with out-of-plane C–H bending modes of meta-, para-, and ortho-substituted aromatic rings. Therefore, for the PPF synthesized at 300 W, the structure is rather represented as a cross-linked alkyl network where variously substituted benzene rings are incorporated. With higher energy input, the balance of fragmentation products shifts from initially abundant aromatic free radicals to small-molecular aliphatic free radicals that undergo random polyrecombination with each other and with the remaining ring moieties. Together with the interaction of the growing film front with more energetic plasma particles and possible cross-cycle reactions, this leads to the deposition of a branched and cross-linked three-dimensional networks with a polystyrene-type backbone. Notably absent in the ex situ spectra are the characteristic absorptions of alkynes, although acetylenic species were found to form in plasma during fragmentation at higher powers. Suggestedly, acetylene takes an active part in recombination reactions. For example, an aromatic ring with two radicals at ortho positions (energy cost of  $\sim 7.8$  eV, see Figure 3) might undertake an electrophilic attack on the triple bonds of two acetylene molecules, resulting in the ring closure and the formation of a naphthalene species through the H-abstraction– $\text{C}_2\text{H}_2$ -addition (HACA) mechanism.<sup>40,41</sup> Alternatively, the interaction of benzene and acetylene, one or both in reactive states, could generate a styrene-like moiety with a double bond capable of initiating free radical grafting polymerization (to a limited degree due to a highly agitated and manifold plasma environment).<sup>38</sup> The broadening of FTIR bands in comparison to the respective counterparts in conventional organic compounds is a well-

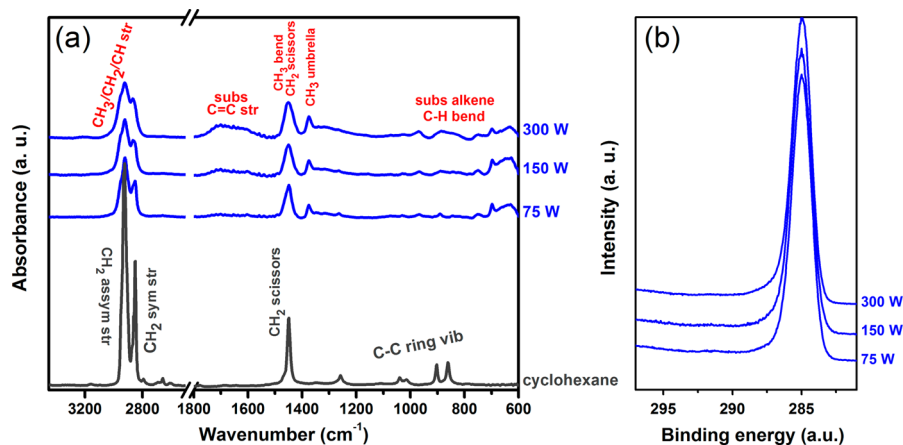


**Figure 6.** Ex situ FTIR (a) and C 1s XPS (b) spectra for the cyclohexane-based PPF synthesized at different deposition powers.

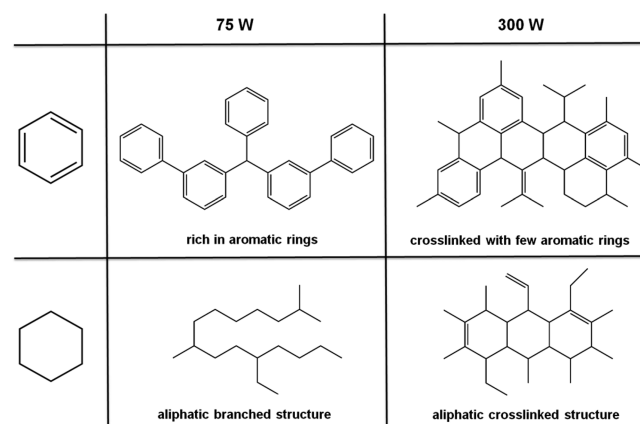
known feature<sup>42,43</sup> caused by the plasma polymerization specifics when branching and cross-linking results in the superposition of vibration modes. In summary, the ex situ FTIR analysis of the PPF is in good agreement with the in situ plasma FTIR analysis both suggesting the decrease in aromaticity in favor of aliphatic structural moieties for the benzene plasma and for the corresponding PPF with power and linking, thus, together plasma phase and deposited material characterizations. These findings are further supported by XPS data (Figure 5b), C 1s peak of the benzene-based PPF displays along with the main C peak at ~285 eV, attributed to the aliphatic component of the C–C bond, a rather broad shakeup feature at ~292 eV. This feature is often considered to be characteristic of aromatic compounds because it arises from the inelastic loss process that excites the ground-state  $\pi$  orbitals ( $\pi \rightarrow \pi^*$  transitions).<sup>44–46</sup> The decrease in the shakeup satellite with power implies that the benzene-based PPF is losing aromaticity in favor of alkyl bonds with the higher energy input. For low deposition powers, free radicals on the surface of the PPF are mainly located on the edges of aromatic rings whereas for the higher powers, the expanded cross-linked aliphatic network would additionally give rise to midchain/endchain alkyl radicals that can be further stabilized when located in the proximity of conjugated structures.

Figure 6 shows ex situ FTIR and XPS spectra of the cyclohexane-based PPF deposited with input powers of 75, 150, and 300 W.

The ex situ FTIR spectrum of the cyclohexane-based PPF deposited at 75 W exhibits in the wavenumbers of the original alkane CH<sub>2</sub> vibrations growing contributions around ~2960 and ~2872 cm<sup>-1</sup> representative of CH<sub>3</sub> asymmetric/symmetric stretch, the appearance of new bands attributed to CH<sub>3</sub> bending modes (~1450 and 1375 cm<sup>-1</sup>) superimposed on CH<sub>2</sub> scissors (~1450 cm<sup>-1</sup>) and the disappearance of the C–C aliphatic ring vibrations (850–1050 cm<sup>-1</sup>). These changes support the massive cyclohexane ring opening fragmentation pattern, suggested by the plasma FTIR spectroscopy and DFT calculations, leading to the formation of a cross-linked alkyl network. With higher powers, the main PPF peaks are further broadened due to the increased branching and cross-linking originating from the stronger fragmentation in plasma and from the interaction of the growing polymer with more energetic plasma particles. The observation of new broad bands (consisting of the superposition of many small peaks) in the group wavenumbers of substituted alkene C–C stretch (1600–

1780 cm<sup>-1</sup>) and C–H bend (700–1000 cm<sup>-1</sup>) points to an increasing fraction of double bonds in the synthesized plasma polymer with power. Unsaturation might additionally arise from photoinitiated reaction in the bulk of the growing film as the vacuum ultraviolet (VUV) radiation intensifies.<sup>47,48</sup> The absence of the  $\pi \rightarrow \pi^*$  transition peak on the C 1s XPS spectra for all powers (Figure 6b) confirms the expected absence of aromatic structures in the cyclohexane-based PPF constituted by predominantly aliphatic C–C bonds, as also indicated by FTIR. Carbon atoms in this cross-linked hydrocarbon network, increasing its degree of unsaturation with power, give rise to mainly midchain/endchain alkyl and allyl radicals on the PPF surface.

Bringing together FTIR and XPS findings, a structure model for both PPF synthesized at extreme powers is proposed in Figure 7. It may serve for a better understanding of the surface free radical density changes addressed henceforth.



**Figure 7.** Schematic structures of PPF synthesized, respectively, from benzene and cyclohexane at 75 and 300 W.

Structural differences can be correlated with the mechanism of the plasma polymer formation, namely, the plasma-induced grafting of aromatic species and the extensive polyrecombination of unsaturated fragments for benzene against merely polyrecombination of aliphatic fragments in the case of cyclohexane. As it can be seen, the magnitude of aromaticity retention in the synthesized PPF can be tuned with power. Therefore, the following section deals with the effect of

aromaticity on the concentration and stability of surface free radicals important for any subsequent chemical modification.

**Surface Free Radicals.** The evaluation of the density of free radicals on the surface of the PPF has been performed with the help of NO chemical derivatization in combination with XPS analysis according to the procedure established and reported elsewhere.<sup>20,25</sup> The values of free radical density have been determined from the atomic concentration of nitrogen, derived from the XPS N 1s peak, using the following formula:

$$[\text{spin}] = \text{at.\%N} \cdot N_A \cdot \frac{\rho}{M} \cdot l \quad (1)$$

where at. % N is the concentration of nitrogen in at. %,  $N_A$  is the Avogadro constant in  $\text{mol}^{-1}$ ,  $M$  is the molar mass of nitrogen in  $\text{g}\cdot\text{mol}^{-1}$ ,  $\rho$  is the density of PPF in  $\text{g}\cdot\text{cm}^{-3}$  and  $l$  is the XPS analysis depth in cm. The calculation was carried out assuming the plasma polymer density of  $0.9 \text{ g}\cdot\text{cm}^{-3}$ .<sup>23</sup> The dependency of the surface free radical density on the deposition power for both PPF is presented in Figure 8. The spin concentration is therefore expressed in number of spins per  $\text{cm}^2$ .

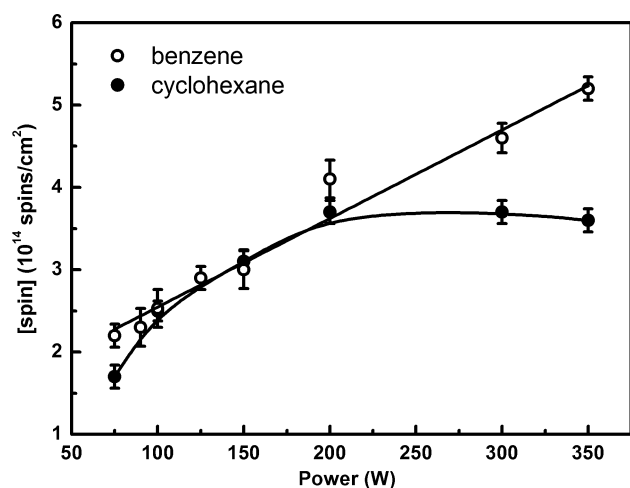


**Figure 8.** Surface free radical density as a function of power for benzene- and cyclohexane-based PPF.

Figure 8 shows that for the benzene-based PPF, the free radical density exhibits a linear rise in the entire studied power range (75–350 W) whereas for the cyclohexane-based PPF, it stabilizes to a plateau after ca. 200 W. In both cases, initially the increasing power causes the intensification of phenomena such as the precursor fragmentation in plasma, the interaction of the growing PPF front with plasma particles, and the vacuum ultraviolet (VUV) radiation. In turn, this leads to increased C–H and C–C bond scissions, producing higher amounts of free radicals. For the cyclohexane molecules, which are devoid of the resonance-induced stability and hence require less energy to break up the saturated C–C ring, the stabilization of alkyl/allyl radical density above 200 W does not support the concept of the energy-deficient domain where the polymer-forming free radicals should progressively increase their concentration in plasma. The entire power range studied for both benzene and cyclohexane precursors lies in the energy-deficient domain<sup>49</sup> where the degree of fragmentation, directly related with the polymer-forming free radical density, and hence the deposition rate (given in the Supporting Information), are dependent on the energy input. Its increase causes intramolecular bonds in

the initial precursor molecule to break progressively, leading to the rising amount of free radical species in plasma available for polymer synthesis and consequently trapped in it. The inconsistency can be probably explained by recombination reactions between free radicals on the surface of the PPF. Calculating (with the help of formula 1 by considering 100% of carbon atoms for the PPF based on cyclohexane and benzene), the average carbon atoms density of  $\sim 10^{16} \text{ at./cm}^2$  and taking into account that the cross-linked PPF is mainly constituted by the variation of C–C bonds, the mean distance between derivatized radicals is estimated to be in the order of a few nanometers. Deposition powers above 200 W supposedly give rise to a higher number of surface free radicals with correspondingly smaller spacing between them. These abundant closely located radicals, which are as well allowed a certain (restricted) mobility on the surface of the cross-linked PPF, might undergo recombination reactions if the spacing between them is not large enough to prevent recombination. Therefore, the stabilization of free radical density for a minimum noninteracting radical distance is reflected in NO chemical labeling experiments as a plateau of the detected surface free radical density at higher powers.

For the benzene-based PPF, the entire studied power range also remains in the energy-deficient domain. However, the extensive opening of the aromatic ring and its breaking into small-molecular alkyl fragments for the benzene precursor would require higher energy inputs due to the resonance-induced stability. The retention of aromaticity in the PPF observed by both in situ and ex situ FTIR as well as by XPS supports the idea that the complete fragmentation is yet to be reached. Additionally, benzene contains unsaturated bonds that might serve as an extra source of free radicals upon ring disintegration as compared to the saturated cyclohexane molecule. The surface of this PPF can accumulate more free radicals with a minimum noninteracting distance due to the additional stability against recombination induced by the presence of aromatic rings in the intermolecular neighborhood. The free radical stability increases when its electron pull is subdued by the nearby structure with delocalized electrons.<sup>15,28</sup>

This is likely to be the reason why for the powers where for the cyclohexane-based PPF, free of regularly connected conjugated fragments, the surface free radical density is stabilized due to recombination reactions, for the benzene-based PPF it continues to grow. The difference in the surface free radical density is associated with different fragmentation patterns, radical generation, and plasma polymer formation mechanisms for each of the precursors and can serve as a practical initial guide for the subsequent surface functionalization.

In connection with the free radical evolution, the oxidation of the PPF, also known as aging,<sup>13,14</sup> has been addressed through the investigation of the oxygen uptake, deduced from the corresponding O 1s XPS spectra, upon exposure to air and is presented in Figure 9.

Free radicals, present on the surface of any plasma polymer, undergo reactions with omnipresent oxygen molecules once the sample is removed from the vacuum chamber into the ambient. The well-known autoxidation process<sup>15</sup> is assumed to begin with the prompt formation of peroxy radicals through the reactions of carbon-centered radicals with  $\text{O}_2$  followed by the H abstraction to form hydroperoxides. In turn, unstable hydroperoxides generate on longer time scales new reactive free radical species capable of introducing various oxygen functionalities on the PPF surface, thus resulting in the random

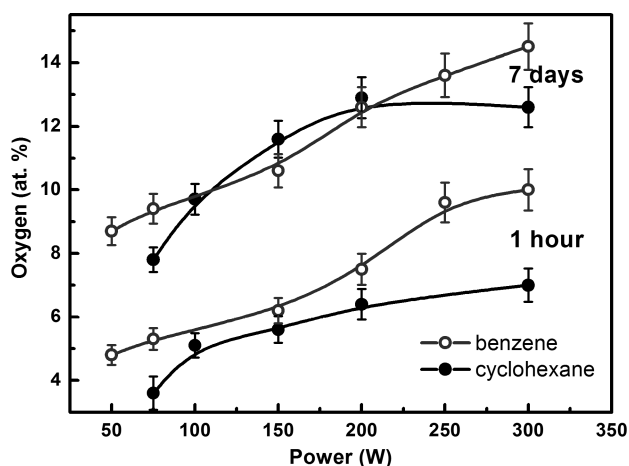


**Figure 9.** Oxygen uptake of the benzene- and cyclohexane-based PPF measured as a function of deposition power after 1 and 7 days of aging.

surface functionalization. Due to the nonlinear character of autoxidation, each carbon-centered free radical, available for a reaction with  $O_2$ , might accumulate along with the initial oxygen atom a few additional oxygen atoms in time.

After 1 h of exposure to air, both the benzene- and cyclohexane-based PPF exhibit an increase of oxygen content on the surface with deposition power attributed to the formation of peroxy radicals and hydroperoxides from initial carbon-centered free radicals. This dependency repeats the trend of the plots of surface free radical density against power, a growing concentration of radicals with power gives rise to a higher oxygen uptake. For the cyclohexane-based PPF, a plateau of oxygen uptake at elevated powers can be explained by the stabilization of the free radical density due to recombination reactions. The benzene-based PPF demonstrates a higher overall oxygen uptake at elevated powers due to the increased free radical amount, providing more potential sites for termination reactions with oxygen. Though the resonance-induced stability of free radicals in the benzene-based PPF appears to be sufficient enough to prevent radical recombination in anaerobic conditions, it cannot efficiently resist against reactive oxygen molecules under ambient atmosphere.

Both PPF left for 1 week in air continued to accumulate oxygen on their surface, as indicated by a considerable increase in oxygen uptake values. Their respective shapes as a function of the input power repeat the initial shapes because after the relatively quick hydroperoxide formation, the same original free radical centers can incorporate up to a few additional oxygen atoms on a longer time scale of autoxidation.

Along with oxygen uptake experiments, another series of aging tests provided additional information on the free radical decay upon contact with air. PPF samples, deposited at three selected powers from both precursors, were left over different time intervals in the ambient atmosphere and only then were they derivatized with nitric oxide in order to highlight the fraction of surviving free radicals. This data, presented as the nitrogen content, derived from the XPS N 1s spectra, is given in Figure 10 as a function of the aging duration.

The dependency is intentionally presented along the *y*-axis as the atomic concentration of nitrogen atoms determined from N 1s XPS spectra, and not as the converted free radical density (see justification hereafter). The values at 0 days are associated with the initial concentration of surface free radicals in PPF after the depositions when the samples were kept in vacuum

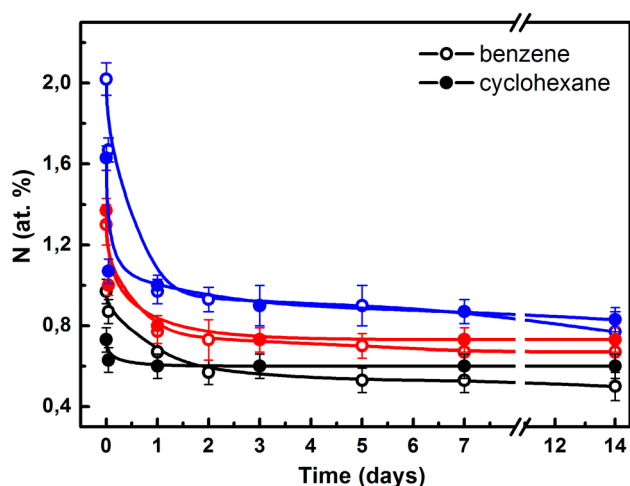


**Figure 10.** Nitrogen content on the surface of the benzene- and cyclohexane-based PPF after NO derivatization, deposited at 75 (black), 150 (red), and 300 W (blue), as a function of the air exposure time.

without contact with the ambient atmosphere. As it can be seen after 1 h of air exposure, the surface free radical density is reasonably decreased with a more noticeable reduction for higher deposition powers (powers that gave rise to a higher initial radical concentration). However, storage for 1 day and longer in aerobic conditions causes the leveling of the free radical concentration to a stable plateau, implying that the radicals in reactive sites accessible to oxygen molecules have undergone corresponding autoxidation reactions. The last statement is rather debatable because various oxygen containing surface functional groups formed upon contact with air might undergo side reactions with NO, leading to the overestimation of free radical density when addressed by chemical derivatization.<sup>15</sup> This is the reason for presenting the data along the *y*-axis as the nitrogen content rather than as the associated surface free radical density. However, the leveling of the free radical signal with exposure time has already been reported.<sup>16</sup> It was attributed to the migration of free radicals from their reservoir under the surface, constituted by the radicals trapped in the bulk of the plasma polymer during synthesis, in the response to free radical density reduction on the surface.<sup>50</sup> It is worth noting that independent of the relative stability of the carbon-centered radical type, aromatic or resonance-stabilized radicals in the benzene-based PPF or alkyl/allyl radicals in the cyclohexane-based PPF, they all undergo quenching reactions with oxygen molecules once removed from the vacuum chamber, provided that these molecules can reach the free radical center.

The aging tests have thus revealed that when the surface free radicals in the PPF are intended to be used for grafting of a specific chemical group or molecule with a purpose of a controlled surface functionalization, air exposure should be avoided and the subsequent grafting should be performed under anaerobic conditions. Otherwise, surface free radicals undergo manifold autoxidation reactions with  $O_2$  in the ambient, generating a randomly functionalized, oxygen-rich surface poorly suitable for further uniform chemical modifications.



## CONCLUSIONS

PPF were synthesized from benzene and cyclohexane precursors by the PECVD technique in order to study the effect of aromaticity on the free radical generation and concentration considering the importance of free radicals for a successful subsequent surface functionalization. In situ FTIR spectroscopy of the plasma phase, supplemented by DFT calculations, allowed us to shed light on the main fragmentation routes of precursors in plasma: activation of benzene rings and their partial disintegration into predominantly acetylenic intermediates versus breaking of cyclohexane molecules into relatively long hydrocarbon fragments. Plasma polymers, deposited at selected powers corresponding to minor, medium, and strong fragmentation in plasma, were characterized by ex situ FTIR and XPS. The findings suggest that, in the case of the benzene precursor, the aromaticity is retained in the PPF to an extent depending on the power. For the 75 W deposition power, the structure is rather represented as benzene rings joined randomly by short alkyl bridges, whereas for the highest energy input, 300 W, it changes to a more extensively cross-linked alkyl network where a few aromatic rings are incorporated. The cyclohexane-based PPF exhibits a branched aliphatic structure that increases its degree of unsaturation and cross-linking with power. For benzene, partial plasma-induced graft polymerization of activated rings has been proposed as the polymer formation mechanism in addition to the polyrecombination of reactive predominantly acetylenic intermediates. Whereas for cyclohexane, predominantly polyrecombination of relatively long alkyl molecular fragments should be considered. NO chemical labeling, in combination with a subsequent XPS analysis, allowed us to quantitatively estimate the density of surface free radicals in plasma polymers as a function of input power and, hence, aromaticity retention. The benzene-based PPF exhibits a linear increase of free radical density (up to  $5 \times 10^{14}$  spin/cm<sup>2</sup>) in the entire power range contrarily to the cyclohexane-based PPF for which a stabilization of the radical density (up to  $3.5 \times 10^{14}$  spin/cm<sup>2</sup>) at powers above 200 W is observed. These differences can be attributed to the relative stabilities of surface free radicals with regard to recombination reactions. For the cyclohexane-based polymer, the cross-linked network allows for recombination reactions between closely located mainly alkyl free radicals to take place, leading to a leveling of their density. However, in the case of the benzene-based polymer, free radicals in the aliphatic network are additionally stabilized by the proximity of resonant structures (incorporated aromatic rings), preventing their reciprocal termination reactions. This work shows on the example of surface free radical study of two counterpart hydrocarbon precursors a functionalization potential of plasma polymers and a way to control it (via aromaticity retention) when the grafting of a chemical functionality on the PPF is intended.

Aging experiments, including oxygen uptake and derivatization study after air exposure, indicate that postoxidation reactions play an important role in the quenching of surface free radicals, otherwise potentially available for grafting. Their quantity rapidly decreases in the ambient and stabilizes after 1 day of exposure, suggesting that most free radicals accessible to oxygen molecules have undergone a terminations reaction with O<sub>2</sub> molecules by then. On a longer time-scale, the PPF surface gets further enriched in oxygen due to the capacity of initially formed oxygen-containing groups to incorporate more oxygen

atoms. Therefore, when surface functionalization of the plasma polymer is considered, air exposure should be avoided in order to achieve an efficient and controlled grafting.

## ASSOCIATED CONTENT

### Supporting Information

Description of in situ FTIR measurements and deposition rate plot. This material is available free of charge via the Internet at <http://pubs.acs.org>.

## AUTHOR INFORMATION

### Corresponding Author

\*R. Snyders. E-mail: [rony.snyders@umons.ac.be](mailto:rony.snyders@umons.ac.be).

### Present Address

<sup>1</sup>Department of Advanced Materials and Structures, Public Research Centre Henri Tudor, avenue J.F. Kennedy 29, 1855 Luxembourg City, Luxembourg.

### Notes

The authors declare no competing financial interest.

## ACKNOWLEDGMENTS

This work is supported by the Belgian Government through the 'Pôle d'Attraction Interuniversitaire' (PAI, P7/34, "Plasma-Surface Interaction", Ψ). The Walloon Region and the European Commission are also thanked for financial support through the Feder Project "SURFACE" and the "Opti2mat" program.

## ABBREVIATIONS

- ATR, attenuated total reflection
- CAE, constant analyzer energy
- CAP, competitive ablation polymerization
- DFT, density functional theory
- DPPH, di(phenyl)-(2,4,6-trinitrophenyl)iminoazanium
- ESR, electron spin resonance
- FTIR, Fourier transform infrared spectroscopy
- HACA, H-abstraction-C<sub>2</sub>H<sub>2</sub>-addition
- NO, nitric oxide
- PECVD, plasma-enhanced chemical vapor deposition
- PPF, plasma polymer film(s)
- VUV, vacuum ultraviolet
- XPS, X-ray photoelectron spectroscopy

## REFERENCES

- (1) Muguruma, H. Plasma-Polymerized Films for Biosensors II. *TrAC, Trends Anal. Chem.* **2007**, *26*, 433–443.
- (2) Förch, R.; Zhang, Z.; Knoll, W. Soft Plasma Treated Surfaces: Tailoring of Structure and Properties for Biomaterial Applications. *Plasma Processes Polym.* **2005**, *2*, 351–372.
- (3) Siow, K. S.; Britcher, L.; Kumar, S.; Griesser, H. J. Plasma Methods for the Generation of Chemically Reactive Surfaces for Biomolecule Immobilization and Cell Colonization - A Review. *Plasma Processes Polym.* **2006**, *3*, 392–418.
- (4) Theapsak, S.; Watthanaphanit, A.; Rujiravanit, R. Preparation of Chitosan-Coated Polyethylene Packaging Films by DBD Plasma Treatment. *ACS Appl. Mater. Interfaces* **2012**, *4*, 2474–2482.
- (5) Hamilton-Brown, P.; Gengenbach, T.; Griesser, H. J.; Meagher, L. End Terminal, Poly(Ethylene Oxide) Graft Layers: Surface Forces and Protein Adsorption. *Langmuir* **2009**, *25*, 9149–9156.
- (6) Zhang, Z.; Chen, Q.; Knoll, W.; Foerch, R.; Holcomb, R.; Roitman, D. Plasma Polymer Film Structure and DNA Probe Immobilization. *Macromolecules* **2003**, *36*, 7689–7694.
- (7) Yasuda, H. Glow Discharge Polymerization. *J. Polym. Sci. Macromol. Rev.* **1981**, *16*, 199–293.

- (8) Yasuda, H. *Plasma Polymerization*; Academic Press: Orlando, FL, 1985.
- (9) Yasuda, H.; Yasuda, T. Competitive Ablation and Polymerization (CAP) Principle and the Plasma Sensitivity of Elements in Plasma Polymerization and Treatment. *J. Polym. Sci., Part A: Polym. Chem.* **2000**, *38*, 943–953.
- (10) Friedrich, J. Mechanisms of Plasma Polymerization—Reviewed from a Chemical Point of View. *Plasma Processes Polym.* **2011**, *8*, 783–802.
- (11) Denis, L.; Cossement, D.; Godfroid, T.; Renaux, F.; Bittencourt, C.; Snyders, R.; Hecq, M. Synthesis of Allylamine Plasma Polymer Films: Correlation between Plasma Diagnostic and Film Characteristics. *Plasma Processes Polym.* **2009**, *6*, 199–208.
- (12) Alexander, M. R.; Duc, T. M. A Study of the Interaction of Acrylic Acid/1,7-Octadiene Plasma Deposits with Water and Other Solvents. *Polymer* **1999**, *40*, 5479–5488.
- (13) Swaraj, S.; Oran, U.; Lippitz, A.; Friedrich, J. F.; Unger, W. E. S. Aging of Plasma-Deposited Films Prepared from Organic Monomers. *Plasma Processes Polym.* **2007**, *4*, S784–S789.
- (14) Gengenbach, T. R.; Chatelier, R. C.; Griesser, H. J. Characterization of the Ageing of Plasma-Deposited Polymer Films: Global Analysis of X-Ray Photoelectron Spectroscopy Data. *Surf. Interface Anal.* **1996**, *24*, 271–281.
- (15) Meyer-Plath, A. Identification of Surface Radicals on Polymers. *Vak. Forsch. Prax.* **2005**, *17*, 40–46.
- (16) Yamauchi, Y.; Sasai, Y.; Kondo, S.-i.; Kuzuya, M. Chemical Diagnosis of DLC by ESR Spectral Analysis. *Thin Solid Films* **2010**, *518*, 3492–3496.
- (17) Wavhal, D. S.; Fisher, E. R. Membrane Surface Modification by Plasma-Induced Polymerization of Acrylamide for Improved Surface Properties and Reduced Protein Fouling. *Langmuir* **2003**, *19*, 79–85.
- (18) Wavhal, D. S.; Fisher, E. R. Hydrophilic Modification of Polyethersulfone Membranes by Low Temperature Plasma-Induced Graft Polymerization. *J. Membr. Sci.* **2002**, *209*, 255–269.
- (19) Teare, D. O. H.; Schofield, W. C. E.; Garrod, R. P.; Badyal, J. P. S. Rapid Polymer Brush Growth by Tempo-Mediated Controlled Free-Radical Polymerization from Swollen Plasma Deposited Poly-(Maleic Anhydride) Initiator Surfaces. *Langmuir* **2005**, *21*, 10818–10824.
- (20) Khelifa, F.; Ershov, S.; Habibi, Y.; Snyders, R.; Dubois, P. Use of Free Radicals on the Surface of Plasma Polymer for the Initiation of a Polymerization Reaction. *ACS Appl. Mater. Interfaces* **2013**, *5*, 11569–11577.
- (21) Teng, R.; Yasuda, H. K. Ex Situ Chemical Determination of Free Radicals and Peroxides on Plasma Treated Surfaces. *Plasmas Polym.* **2002**, *7*, 57–69.
- (22) Kuzuya, M.; Yamashiro, T.; Kondo, S. I.; Sugito, M.; Mouri, M. Plasma-Induced Surface Radicals of Low-Density Polyethylene Studied by Electron Spin Resonance. *Macromolecules* **1998**, *31*, 3225–3229.
- (23) Wilken, R.; Holländer, A.; Behnisch, J. Nitric Oxide Radical Trapping Analysis on Vacuum-Ultraviolet Treated Polymers. *Macromolecules* **1998**, *31*, 7613–7617.
- (24) Wilken, R.; Holländer, A.; Behnisch, J. Surface Radical Analysis on Plasma-Treated Polymers. *Surf. Coat. Technol.* **1999**, *116–119*, 991–995.
- (25) Ershov, S.; Khelifa, F.; Dubois, P.; Snyders, R. Derivatization of Free Radicals in an Isopropanol Plasma Polymer Film: The First Step toward Polymer Grafting. *ACS Appl. Mater. Interfaces* **2013**, *5*, 4216–4223.
- (26) Kondyurin, A.; Naseri, P.; Fisher, K.; McKenzie, D. R.; Bilek, M. M. Mechanisms for Surface Energy Changes Observed in Plasma Immersion Ion Implanted Polyethylene: The Roles of Free Radicals and Oxygen-Containing Groups. *Polym. Degrad. Stab.* **2009**, *94*, 638–646.
- (27) Kuzuya, M.; Noguchi, A.; Ito, H.; Kondo, S.-I.; Noda, N. Electron Spin Resonance Studies of Plasma-Induced Polystyrene Radicals. *J. Polym. Sci., Polym. Chem.* **1991**, *29*, 1–7.
- (28) Kosobrodova, E. A.; Kondyurin, A. V.; Fisher, K.; Moeller, W.; McKenzie, D. R.; Bilek, M. M. Free Radical Kinetics in a Plasma Immersion Ion Implanted Polystyrene: Theory and Experiment. *Nucl. Instrum. Methods Phys. Res., Sect. B* **2012**, *280*, 26–35.
- (29) Denis, L.; Marsal, P.; Olivier, Y.; Godfroid, T.; Lazzaroni, R.; Hecq, M.; Cornil, J.; Snyders, R. Deposition of Functional Organic Thin Films by Pulsed Plasma Polymerization: A Joint Theoretical and Experimental Study. *Plasma Processes Polym.* **2010**, *7*, 172–181.
- (30) Ligot, S.; Guillaume, M.; Gerbaux, P.; Thiry, D.; Renaux, F.; Cornil, J.; Dubois, P.; Snyders, R. Combining Mass Spectrometry Diagnostic and DFT Calculations to Get a Better Understanding of the Plasma Polymerization of Ethyl Lactate. *J. Phys. Chem. B* **2014**, *118*, 4201–4211.
- (31) *Gaussian 09*, Revision C.01; Gaussian, Inc.: Wallingford, CT, 2010.
- (32) Briggs, D.; Seah, P. *Practical Surface Analysis: Auger and X-Ray Photoelectron Spectroscopy*, 2nd ed; John Wiley and Sons: Chichester, U. K., 1990.
- (33) Smith, B. C. *Infrared Spectral Interpretation: A Systematic Approach*; CRC Press: Boca Raton, FL, 1998.
- (34) Socrates, G. *Infrared and Raman Characteristic Group Frequencies: Tables and Charts*, 3rd ed; John Wiley & Sons: Chichester, U. K., 2004.
- (35) Coates, J. Interpretation of Infrared Spectra, a Practical Approach. In *Encyclopedia of Analytical Chemistry*; Meyers, R. A., Ed.; John Wiley & Sons: New York, 2006.
- (36) Thiry, D.; Britun, N.; Konstantinidis, S.; Dauchot, J.-P.; Denis, L.; Snyders, R. Altering the Sulfur Content in the Propanethiol Plasma Polymers Using the Capacitive-to-Inductive Mode Transition in Inductively Coupled Plasma Discharge. *Appl. Phys. Lett.* **2012**, *100*, 071604.
- (37) Inagaki, N. *Plasma Surface Modification and Plasma Polymerization*; Technomic Publishing Company: Lancaster, PA, 1996.
- (38) Neiswender, D. In *Chemical Reactions in Electrical Discharges*, Blaustein, B. D., Ed.; American Chemical Society: Washington, DC, 1969; Chapter 29, pp 338–349.
- (39) Shih, S. I.; Lin, T. C.; Shih, M. Decomposition of Benzene in the Rf Plasma Environment: Part I. Formation of Gaseous Products and Carbon Depositions. *J. Hazard. Mater.* **2004**, *116*, 239–248.
- (40) Shih, S. I.; Lin, T. C.; Shih, M. Decomposition of Benzene in the RF Plasma Environment: Part II. Formation of Polycyclic Aromatic Hydrocarbons. *J. Hazard. Mater.* **2005**, *117*, 149–159.
- (41) Bauschlicher, C. W., Jr; Ricca, A. Mechanisms for Polycyclic Aromatic Hydrocarbon (PAH) Growth. *Chem. Phys. Lett.* **2000**, *326*, 283–287.
- (42) Aparicio, F. J.; Blaszczyk-Lezak, I.; Sánchez-Valencia, J. R.; Alcaire, M.; González, J. C.; Serra, C.; González-Elipe, A. R.; Barranco, A. Plasma Deposition of Perylene-Adamantane Nanocomposite Thin Films for NO<sub>2</sub> Room-Temperature Optical Sensing. *J. Phys. Chem. C* **2012**, *116*, 8731–8740.
- (43) Aparicio, F. J.; Borrás, A.; Blaszczyk-Lezak, I.; Gröning, P.; Álvarez-Herrero, A.; Frenández-Rodríguez, M.; González-Elipe, A. R.; Barranco, A. Luminescent and Optical Properties of Nanocomposite Thin Films Deposited by Remote Plasma Polymerization of Rhodamine 6G. *Plasma Processes Polym.* **2009**, *6*, 17–26.
- (44) Mackie, N. M.; Castner, D. G.; Fisher, E. R. Characterization of Pulsed-Plasma-Polymerized Aromatic Films. *Langmuir* **1998**, *14*, 1227–1235.
- (45) Asandulesa, M.; Topala, I.; Pohoata, V.; Legrand, Y. M.; Dobromir, M.; Totolin, M.; Dumitrascu, N. Chemically Polymerization Mechanism of Aromatic Compounds under Atmospheric Pressure Plasma Conditions. *Plasma Processes Polym.* **2013**, *10*, 469–480.
- (46) Jiang, H.; Hong, L.; Venkatasubramanian, N.; Grant, J. T.; Eyink, K.; Wiacek, K.; Fries-Carr, S.; Enlow, J.; Bunning, T. J. The Relationship between Chemical Structure and Dielectric Properties of Plasma-Enhanced Chemical Vapor Deposited Polymer Thin Films. *Thin Solid Films* **2007**, *515*, 3513–3520.
- (47) Holländer, A.; Wilken, R.; Behnisch, J. Subsurface Chemistry in the Plasma Treatment of Polymers. *Surf. Coat. Technol.* **1999**, *116–119*, 788–791.

(48) Wilken, R.; Holländer, A.; Behnisch, J. Vacuum Ultraviolet Photolysis of Polyethylene, Polypropylene, and Polystyrene. *Plasma Polym.* **2002**, *7*, 185–205.

(49) Gilliam, M. A.; Yu, Q.; Yasuda, H. Plasma Polymerization Behavior of Fluorocarbon Monomers in Low-Pressure AF and RF Discharges. *Plasma Processes Polym.* **2007**, *4*, 165–172.

(50) Bilek, M. M. M.; Bax, D. V.; Kondyurin, A.; Yin, Y.; Nosworthy, N. J.; Fisher, K.; Waterhouse, A.; Weiss, A. S.; Dos Remedios, C. G.; McKenzie, D. R. Free Radical Functionalization of Surfaces to Prevent Adverse Responses to Biomedical Devices. *Proc. Natl. Acad. Sci. U. S. A.* **2011**, *108*, 14405–14410.